ResearchGate

See discussions, stats, and author profiles for this publication at: https://www.researchgate.net/publication/258398573

A Robust Control of Two-Wheeled Mobile Manipulator with Underactuated Joint by Nonlinear Backstepping Method

Article *in* IEEJ Transactions on Industry Applications · June 2010

DOI: 10.1541/ieejias.130.742

CITATIONS
10

READS
904

2 authors, including:

Cihan Acar
Institute for Infocomm Research
7 PUBLICATIONS **72** CITATIONS

SEE PROFILE

All content following this page was uploaded by Cihan Acar on 08 September 2017.

The user has requested enhancement of the downloaded file.

Paper

A Robust Control of Two-Wheeled Mobile Manipulator with Underactuated Joint by Nonlinear Backstepping Method

Cihan Acar* Non-member
Toshiyuki Murakami** Senior Member

In this paper, a robust control of two-wheeled mobile manipulator with underactuated joint is considered. Two-wheeled mobile manipulators are dynamically balanced two-wheeled driven systems that do not have any caster or extra wheels to stabilize their body. Two-wheeled mobile manipulators mainly have an important feature that makes them more flexible and agile than the statically stable mobile manipulators. However, two-wheeled mobile manipulator is an underactuated system due to its two-wheeled structure. Therefore, it is required to stabilize the underactuated passive body and, at the same time, control the position of the center of gravity (CoG) of the manipulator in this system. To realize this, nonlinear backstepping based control method with virtual double inverted pendulum model is proposed in this paper. Backstepping is used with sliding mode to increase the robustness of the system against modeling errors and other perturbations. Then robust acceleration control is also achieved by utilizing disturbance observer. The performance of proposed method is evaluated by several experiments.

Keywords: two-wheeled mobile manipulator, backstepping, sliding mode, disturbance observer, double inverted pendulum.

1. Introduction

Conventional manipulators, which can only be used in factories and industrial environments, are mainly capable of performing tasks such as welding, assembly, painting, polishing, and grinding. They have limited workspaces due to their fixed based structures. It is possible to increase the workspaces of the robot manipulators by combining them with mobile type robots. Because mobile robots are not connected to the fix locations, they have unlimited workspaces. The combination of these robots basically results in mobile manipulators that possess properties of both types of robots.

Unlike conventional manipulators, mobile manipulators can be used in daily life environment (homes, offices, hospitals, etc..) and, hazardous environments. Since mobile manipulators have many degrees of freedom, they are suitable to perform various tasks such as avoidance of obstacles, pushing, picking and placing tasks, opening doors, and etc [?] [?]. Even though bipedal robots are also able to perform these kinds of tasks, their complex structure restricts their usage most of the cases [?]. Wheeled robots, on the other hand, have less complex structures. Thus, it is easier to control them compared to the legged robots.

There are many studies related to mobile manipulators in last several decades. However, these researches are mainly based on mobile manipulators, which have three or more wheels. These robots are statically stable because they do not need any motion to maintain their balance during standing posture. Although they can perform the tasks as mentioned above, the extra wheels or casters mostly prevent their performance and speed.

In addition, these robots should have large bases, that is, footing to compensate the manipulator motion, keep from falling over, and handle the heavy payloads. On the other hand, mobile manipulators need to have similar or smaller footing than human in order to operate in the human environment easily. Manipulation at human level requires the mobile manipulator to have a high CoG but having a high CoG may make it unstable against unexpected external forces.

Using two wheels without any casters or wheels for the mobile platform changes the characteristic of the systems dramatically. The Segway and Segway Robotic Mobility Platform (RMP) are well-known examples of two-wheeled mobile platforms [?]. Different control structures such as partial feedback linearization [?] and linear quadratic regulator (LQR) [?] are applied to control the two-wheeled mobile systems.

Two-wheeled mobile manipulators can have smaller footing than statically stable mobile manipulators. They are also more flexible and maneuverable compared to the statically stable mobile manipulators. In addition to this, they are more sensitive against the unexpected external forces due to their dynamic stability. For instance, an external force in the lateral direction causes the robot to change its position in order to remain stable. This behavior, similar to the compliance motion, decreases the impact force and the damage received by

* Department of System Design Engineering, Keio University, Yokohama 223-8522, Japan
** Department of System Design Engineering, Keio University, Yokohama 223-8522, Japan

the system [?]. As a result, they can be used easily in the human environment for human assistance. There are researches considering mobile manipulator systems with Segway RMP mobile platform such as NASA's Robonaut and Cardea that is developed by MIT to perform door opening task [?]. The uBot is other two-wheeled mobile manipulator utilized to show the efficient of the force generation with the dynamic stability [?].

The two-wheeled mobile manipulator systems without any casters are underactuated mechanical systems. In underactuated mechanical systems, there are more degrees of freedom than the number of actuators, which result in second-order nonholonomic constraints and highly nonlinear structure of the system. Thus, it is not possible to control the motion of the passive body(joint) directly in these systems. The linear controller was applied to control the attitude of the two-wheeled underactuated mobile manipulator [?]. However, this method depends on the linearization of dynamic equations around the zero equilibrium point. Because of linearization, the passive joint can be only stabilized around the equilibrium point, which limits the stability and motion of the CoG of the manipulator.

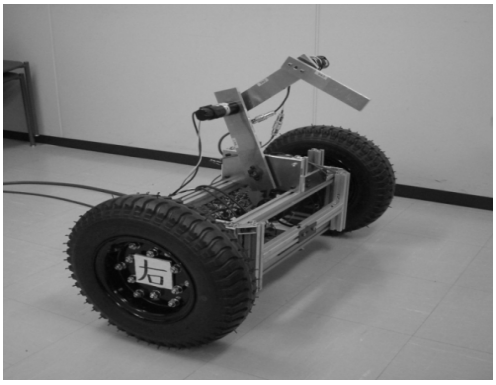

Fig. 1. The Two-Wheeled Mobile Manipulator

In this paper, in order to simply the design and control the CoG of the manipulator, the two-wheeled mobile manipulator as shown in Fig.**??** is modeled as a two-wheeled system with a virtual link that is assumed to composite of the second, third and fourth links of manipulator. This structure is then considered as a double inverted pendulum with a virtual second link and backstepping based nonlinear control design is proposed to regulate and track the motion of the passive joint. Backstepping is based on the systematic construction of Lyapunov functions considering some of the state variables as virtual control inputs [?]-[?]. Instead of linearizing of dynamic equations and using linear controllers, it is possible to increase the stability and performance of the system by this method. Backstepping makes it possible to track the motion of the passive joint precisely so that the CoG of the manipulator can be moved over a greater range of positions. As a result, workspace of the manipulator can be increased.

Whereas using the virtual link simplifies the control structure, it may cause some modeling error and other perturbations as a trade-off. Also, it may not possible to measure the parameters of manipulator that negatively affect the position of CoG calculation and, in turn stability of whole system. Therefore, sliding-mode is added at the final step of backstepping to make the system robust against modeling error and unknown perturbation [?]. Backstepping with sliding-mode control is applied to control the induction motor drive [?] [?], and piezoactuators [?]. In addition, disturbance observer (DOB) [?] is utilized to achieve the robust acceleration based backstepping with sliding mode control. Disturbance observer can estimate the disturbances and, then can be used to cancel out their affects to improve performance of backstepping.

In manipulator control, joint space disturbance observer and workspace disturbance observer [?] are used together to control the CoG of the manipulator. Joint space and workspace disturbance observers can compensate the nonlinear decoupling effects inertial variation, gravity force, coriolis, centrifugal, and other disturbances due to the passive joint, which provides the robust control of the virtual link. Because of the redundancy of the manipulator, manipulability measure [?] is utilized as a performance index to avoid singularities in the null space of the manipulator. Finally, the validity of the proposed method was confirmed by experiments.

2. Modeling

2.1 Model of The Two-Wheeled Mobile Manipulator The dynamic and kinematics models of the two-wheeled mobile manipulator are described in this section. Model and parameter of the two-wheeled mobile manipulator are given in Fig. **??** and Table **??**, respectively. The base of the mobile manipulator is considered as a passive joint. Therefore, the manipulator part consists of the four links and three actuators.

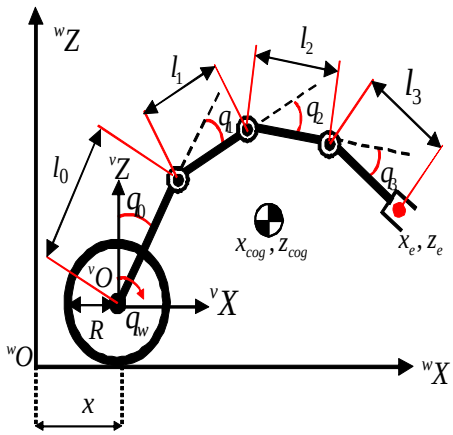

Fig. 2. Model of Two-Wheeled Mobile Manipulator

2.1.1 Dynamics The dynamics of mobile manipulator is described as

$$\boldsymbol{\tau} = \boldsymbol{M}(\boldsymbol{q})\ddot{\boldsymbol{q}} + \boldsymbol{H}(\boldsymbol{q}, \dot{\boldsymbol{q}})\dot{\boldsymbol{q}} + \boldsymbol{g}(\boldsymbol{q}) \cdots\cdots\cdots\cdots (1)$$

where $\boldsymbol{q} = [q_w, q_0, q_1, q_2, q_3]^T \in R^5$ is the vector of generalized coordinates, $\boldsymbol{\tau} = [\tau_w, 0, \tau_1, \tau_2, \tau_3]^T \in R^5$ is the input generalized torque and $\boldsymbol{M} \in R^{5\times5}$, $\boldsymbol{H} \in R^{5\times5}$,

Table 1. Parameters of Two-Wheeled Mobile Manipulator

R	The radius of the wheels
$O-^{w}X^{w}Z$	World coordinate frame
$O-^{v}X^{v}Z$	Mobile manipulator coordinate frame
x_e, z_e	Position of the end-effector
x_{cog}, z_{cog}	Position of the CoG
q_w	Rotation angle of the wheels
q_0	Inclination angle of the base (passive) joint
$q_i (i=1,2,3)$	Joint angles of the links
l_0	Length of the base (passive) joint
$l_i (i=1,2,3)$	Lengths of the links
M	Mass of the wheels
m_0	Mass of the base (passive) joint
$m_i (i=1,2,3)$	Mass of links

$\boldsymbol{g}(\boldsymbol{q})\in R^5$ are the inertia, the centrifugal and coriolis force, and the gravity matrices, respectively.

2.1.2 Kinematics The kinematic relations of the mobile manipulator can be written as

$$\boldsymbol{x} = \boldsymbol{f}(\boldsymbol{q}) \cdots (2)$$
$$\dot{\boldsymbol{x}} = \boldsymbol{J}_{aco}(\boldsymbol{q})\dot{\boldsymbol{q}} \cdots (3)$$
$$\ddot{\boldsymbol{x}} = \boldsymbol{J}_{aco}(\boldsymbol{q})\ddot{\boldsymbol{q}} + \dot{\boldsymbol{J}}_{aco}(\boldsymbol{q})\dot{\boldsymbol{q}} \cdots (4)$$

where $\boldsymbol{f}(\boldsymbol{q})$ is a nonlinear forward kinematics function used to calculate the end-effector position. $\boldsymbol{q}$, $\boldsymbol{x}$, $\boldsymbol{J}_{aco}$ are, respectively, the position in the joint space, position in the workspace, and Jacobian matrix.

Kinematics model and parameters of the two-wheeled mobile base is also given in Fig. **??** and Table **??**, respectively.

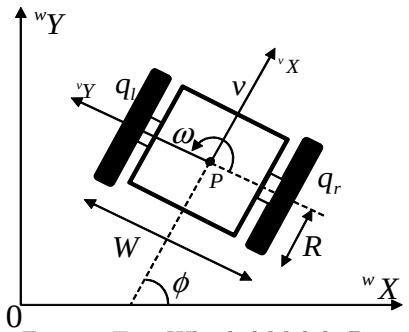

Fig. 3. Two-Wheeled Mobile Base

Table 2. Parameters of Two-Wheeled Mobile Base

$0-^{w}X^{w}Y$	World coordinate frame
$0-^{v}X^{v}Y$	Vehicle coordinate frame
ϕ	Heading angle of the mobile base
W	Tread of the mobile base
q_r	Rotation angle of the right wheel
q_l	Rotation angle of the left wheel
v	Translational velocity of the mobile base
w	Rotational velocity of the mobile base

The kinematics relation between the joint angle velocities of wheels and translation and rotational velocity of the vehicle is defined as

$$\begin{bmatrix} v \\ w \end{bmatrix} = \begin{bmatrix} \frac{R}{2} & \frac{R}{2} \\ \frac{R}{W} & -\frac{R}{W} \end{bmatrix} \begin{bmatrix} \dot{q}_r \\ \dot{q}_l \end{bmatrix}$$

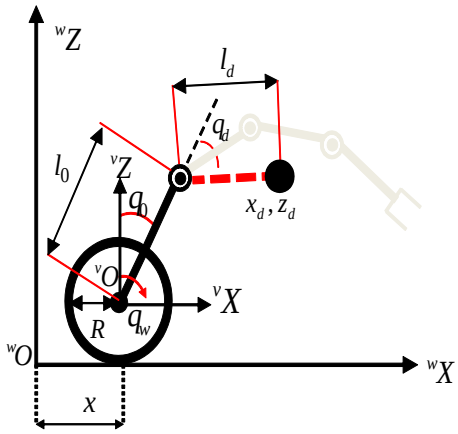

Fig. 4. Virtual Double Inverted Pendulum Model of Two Wheel Mobile Manipulator

$$= \boldsymbol{J}_v\,\dot{\boldsymbol{q}}_{\boldsymbol{w}} \cdots (5)$$

where $\boldsymbol{J}_v\in R^{2\times 2}$ is the Jacobian matrix. By using the inverse jacobian matrix $\boldsymbol{J}_v^{-1}$, joint angle acceleration of the wheels is obtained as

$$\begin{bmatrix} \ddot{q}_r \\ \ddot{q}_l \end{bmatrix} = \begin{bmatrix} \frac{1}{R} & \frac{W}{2R} \\ \frac{1}{R} & -\frac{W}{2R} \end{bmatrix} \begin{bmatrix} \dot{v} \\ \dot{w} \end{bmatrix} \cdots (6)$$

2.2 Double Inverted Pendulum Model It is possible to consider two-wheeled mobile manipulator as a double inverted pendulum with a virtual second link. Fig. **??** shows the model of double inverted pendulum. In this model, the second, third and fourth links of manipulator are considered as the virtual second link of double inverted model. Calculation of positions of the virtual link x_d and z_d, and its length l_d, joint angle q_d, and mass m_d are as follows

$$x_d = \frac{\sum_{i=1}^{3} m_i x_i}{\sum_{i=1}^{3} m_i} \cdots (7)$$
$$z_d = \frac{\sum_{i=1}^{3} m_i z_i}{\sum_{i=1}^{3} m_i} \cdots (8)$$
$$m_d = \sum_{i=1}^{3} m_i \cdots (9)$$
$$l_d = \sqrt{(x_d - x_0)^2 + (z_d - z_0)^2} \cdots (10)$$
$$q_d = \arcsin\left(\frac{x_d - x_0}{l_d}\right) - q_0 \cdots (11)$$

Dynamic equation of this model is obtained by using Euler-Lagrange equation as

$$\boldsymbol{\tau_d} = \overline{\boldsymbol{M}}(\overline{\boldsymbol{q}})\ddot{\overline{\boldsymbol{q}}} + \overline{\boldsymbol{H}}(\overline{\boldsymbol{q}}, \dot{\overline{\boldsymbol{q}}})\dot{\overline{\boldsymbol{q}}} + \overline{\boldsymbol{g}}(\overline{\boldsymbol{q}}) \cdots (12)$$

where $\overline{\boldsymbol{q}} = [q_w, q_0, q_d]^T\in R^3$,$\boldsymbol{\tau}_d = [\tau_w, 0, \tau]^T\in R^3$ are vector of generalized coordinates and input torque vector for the double inverted pendulum model, respectively. $\overline{\boldsymbol{M}}(\overline{\boldsymbol{q}})\in R^{3\times 3}$, $\overline{\boldsymbol{H}}(\overline{\boldsymbol{q}}, \dot{\overline{\boldsymbol{q}}})\in R^{3\times 3}$, $\overline{\boldsymbol{g}}(\overline{\boldsymbol{q}})\in R^3$ matrices are calculated as

$$\overline{\boldsymbol{M}} = \begin{bmatrix} M_{11} & M_{12} & M_{13} \\ M_{21} & M_{22} & M_{23} \\ M_{31} & M_{32} & M_{33} \end{bmatrix},$$

$$\overline{\boldsymbol{H}} = \begin{bmatrix} H_{11} & H_{12} & H_{13} \\ H_{21} & H_{22} & H_{23} \\ H_{31} & H_{32} & H_{33} \end{bmatrix}, \overline{\boldsymbol{g}} = \begin{bmatrix} G_{11} \\ G_{21} \\ G_{31} \end{bmatrix} \cdots (13)$$

where

$$\begin{aligned}
M_{11} &= (M + m_0 + m_d)R^2 \\
M_{22} &= (m_0 + m_d)l_0^2 \\
M_{33} &= m_d l_d^2 \\
M_{12} &= M_{21} = (m_0 + m_d)l_0 R\cos(q_0) \\
M_{13} &= M_{31} = m_d l_d R\cos(q_d) \\
M_{23} &= M_{32} = m_d l_0 l_d \cos(q_0 - q_d) \\
H_{12} &= -(m_0 + m_d)l_0 R\dot{q}_0 \sin(q_0) \\
H_{13} &= -m_d l_d R\dot{q}_d \sin(q_d) \\
H_{23} &= m_d l_0 l_d \dot{q}_d \sin(q_0 - q_d) \\
H_{32} &= -m_d l_0 l_d \dot{q}_0 \sin(q_0 - q_d) \\
G_{21} &= -(m_0 + m_d)g l_0 \sin(q_0) \\
G_{31} &= -m_d g l_d \sin(q_d) \\
H_{11} &= H_{21} = H_{22} = H_{31} = H_{33} = G_{11} = 0
\end{aligned}$$

3. Control System

Since two-wheeled mobile manipulator contains a passive joint, it is required to have an active controller to stabilize this passive joint and control its motion. Unlike statically stable mobile manipulators, stability of passive joint have a crucial effect on stability of the whole system.

This section proposes a nonlinear backstepping based control system to regulate and track the motion of the passive joint. In real systems, it may not be possible to measure the parameters of the system exactly, which causes modeling errors and as a result, degrades stability. In addition, using virtual link model may also cause modeling errors and perturbations. Therefore, it is important to guarantee the stability of the system against modeling errors and other perturbations. To achieve this, sliding mode is used at the final step of backstepping method, which increases the robustness of the system against modeling errors and other perturbations.

3.1 Control of Double Inverted Pendulum Model To control the position of the passive joint, first error variable z_1, its derivative $\dot{z}_1$, and its integral ξ are defined for the first step of backstepping method as follows

$$z_1 = q_0 - q_0^{cmd} \cdots (14)$$
$$\dot{z}_1 = \dot{q}_0 - \dot{q}_0{}^{cmd} \cdots (15)$$
$$\xi = \int_0^t (q_0 - q_0^{cmd})d\tau \cdots (16)$$

In this paper, quadratic Lyapunov function is selected so that recursive procedure of backstepping algorithm becomes easier. In this sense, Lyapunov function candidate for the first error variable is selected as

$$V_1(\xi, z_1) = \frac{1}{2}(\lambda\xi^2 + z_1^2) \cdots (17)$$

where λ is a positive constant design parameter. The derivative of this Lyapunov function is calculated as

$$\begin{aligned}
\dot{V}_1(\xi, z_1) &= \lambda\xi\dot{\xi} + z_1\dot{z}_1 \cdots (18) \\
&= \lambda\xi z_1 + z_1(\dot{q}_0 - \dot{q}_0{}^{cmd})
\end{aligned}$$

If $\dot{q}_0$ were selected as

$$\dot{q}_0 = -\lambda\xi - c_1 z_1 + \dot{q}_0{}^{cmd} \cdots (19)$$

$\dot{V}_1(\xi, z_1)$ becomes negative semi-definite and the error variable z_1 becomes stable as shown in (**??**).

$$\dot{V}_1(\xi, z_1) = -c_1 z_1^2 \leq 0 \cdots (20)$$

Indeed, $\dot{q}_0$ is not an actual control input and cannot be chosen as (**??**). Therefore, virtual control input α is selected as

$$\alpha = -\lambda\xi - c_1 z_1 + \dot{q}_0{}^{cmd} \cdots (21)$$

Difference between the actual and virtual control input is defined as a second error variable z_2, which is given as

$$\begin{aligned}
z_2 &= \dot{q}_0 - \alpha \cdots (22) \\
&= \dot{q}_0 + \lambda\xi + c_1 z_1 - \dot{q}_0{}^{cmd} \cdots (23)
\end{aligned}$$

The new system can be written as below

$$\dot{\xi} = z_1 \cdots (24)$$
$$\dot{z}_1 = -\lambda\xi - c_1 z_1 + z_2 \cdots (25)$$
$$\dot{z}_2 = \ddot{q}_0 - c_1^2 z_1 - c_1\lambda\xi + c_1 z_2 + \lambda z_1 - \ddot{q}_0^{cmd} \cdots (26)$$

To increase the robustness of the system with respect to the unknown perturbation, backstepping is used with sliding-mode controller [7]. Sliding surface is defined as (**??**), which actually equals to the second error variable z_2.

$$\sigma = \dot{q}_0 - \alpha \cdots (27)$$

New Lyapunov function is set as

$$V_2(\xi, z_1, \sigma) = V_1(\xi, z_1) + \frac{1}{2}\sigma^2 \cdots (28)$$

Then the derivative of $V_2(\xi, z_1, \sigma)$ is calculated as

$$\begin{aligned}
\dot{V}_2(\xi, z_1, \sigma) &= \lambda\xi z_1 + z_1\dot{z}_1 + \sigma\dot{\sigma} \cdots (29) \\
&= \lambda\xi z_1 + z_1(\dot{q}_0 - \dot{q}_0{}^{cmd}) \cdots (30) \\
&\quad +\sigma(\ddot{q}_0 - \dot{\alpha}) \\
&= \lambda\xi z_1 + z_1(-\lambda\xi - c_1 z_1 + z_2) \cdots (31) \\
&\quad +\sigma(\ddot{q}_0 + c_1\dot{z}_1 + \lambda z_1 - \ddot{q}_0^{cmd})
\end{aligned}$$

Acceleration of the passive joint $\ddot{q}_0$ is obtained by using the dynamic equation of virtual double inverted pendulum (**??**) as

$$\ddot{q}_0 = \gamma - \beta\ddot{q}_w - \eta \cdots (32)$$

$$\gamma = \frac{g\sin(q_0)}{l_0} \cdots (33)$$
$$\beta = \frac{R\cos(q_0)}{l_0} \cdots (34)$$
$$\eta = \frac{m_d l_d(\cos(q_0 - q_d)\ddot{q}_d + \dot{q}_d\sin(q_0 - q_d))}{(m_0 + m_d)l_0} \cdots (35)$$

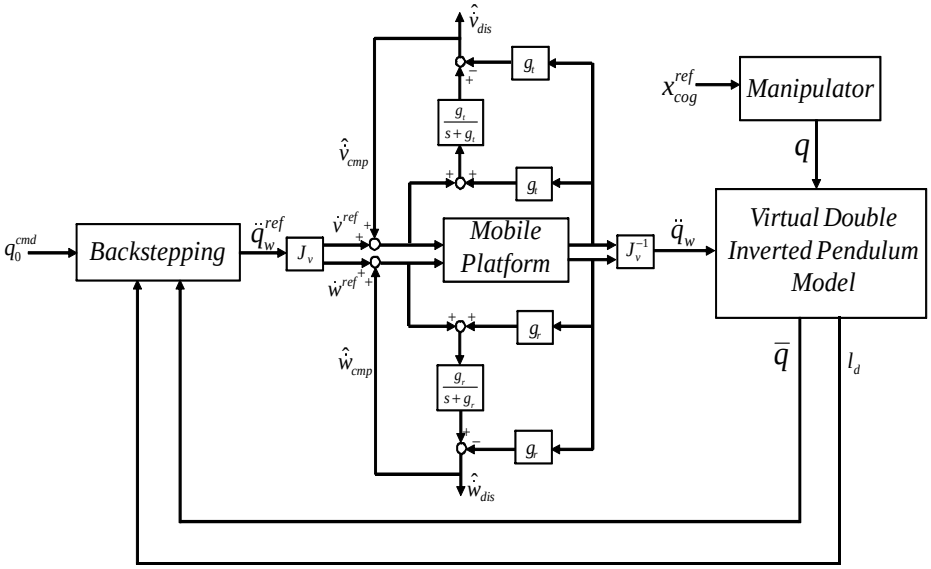

Fig. 5. Block diagram of wheel control

When acceleration input of the wheels $\ddot{q}_w$ are chosen as

$$\ddot{q}_w = \frac{1}{\beta}[\gamma + c_2\sigma + Ksgn(\sigma) + (1+\lambda)z_1 + c_1\dot{z}_1 - \ddot{q}_0^{cmd} - \eta] \cdots\cdots (36)$$

where the terms c_1, c_2 and K are non-negative design parameters and $Ksgn(\sigma)$ is the switching function that deals with the disturbance and dynamic uncertainties, then derivate of the $V_2(\xi, z_1, \sigma)$ becomes negative semi-definite as seen from (**??**), which indicates that V_2 is bounded with the error variables ξ, z_1, and σ.

$$\dot{V}_2(\xi, z_1, \sigma) = -c_1 z_1^2 - c_2\sigma^2 - K|\sigma| \leq 0 \cdots\cdots (37)$$

To show the asymptotical stability of the error variables, W is defined as

$$\dot{V}_2(\xi, z_1, \sigma) \leq -W = -c_1 z_1^2 - c_2\sigma^2 \cdots\cdots (38)$$

Then (**??**) is integrated as

$$\int_0^t W\mathrm{d}t \leq V_2(\xi(0), z_1(0), \sigma(0)) - V_2(\xi(t), z_1(t), \sigma(t)) (39)$$

$$V_2(\xi(t), z_1(t), \sigma(t)) + \int_0^t W\mathrm{d}t \leq V_2(\xi(0), z_1(0), \sigma(0)) (40)$$

$$\int_0^t W\mathrm{d}t \leq V_2(\xi(0), z_1(0), \sigma(0)) (41)$$

Since $V_2(\xi(0), z_1(0), \sigma(0))$ is bounded, (**??**) yields

$$\lim_{t\to\infty}\int_0^t W \leq \lim_{t\to\infty} V_2(\xi(0), z_1(0), \sigma(0)) \leq \infty \cdot (42)$$

which implies that W is bounded According to Barbalat's Lemma [?],

$$\lim_{t\to\infty} W = 0 \cdots\cdots (43)$$

As a result, error variables converge to zero as time goes to infinity and asymptotic stability of the system is guaranteed. Transient performance and convergence time of error variables can be determined and improved by tuning of design parameters c_1 and c_2. By increasing any of these design parameters, performance can be improved. In practical applications, there are disturbances, modeling error and unmodeled dynamics affecting the selection these parameters. Sliding mode and disturbance observer are used to deal with these uncertainties.

Although sliding-mode controller is very efficient against disturbance and parameter variation, using sign function generally causes chattering problem. As a solution, saturation function defined as (**??**) is used to prevent the chattering.

$$sat\left(\frac{\sigma}{\phi}\right) = \begin{cases} \frac{\sigma}{\phi} & if|\frac{\sigma}{\phi}| \leq 1 \\ sgn(\frac{\sigma}{\phi}) & if|\frac{\sigma}{\phi}| > 1 \end{cases} \cdots\cdots (44)$$

where ϕ is the boundary layer thickness and determines the slope of the saturation function. Thus, robustness of systems depends on the width of the boundary.

In the wheel control, disturbance observer is used for the translational and rotational motion to suppress reaction force of the passive joint and other disturbance forces. Fig.**??** shows the structure of the conventional disturbance observer. In this structure, M, K_t, M_n and

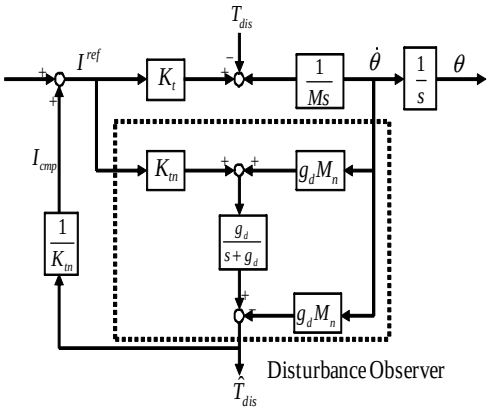

Fig. 6. Block Diagram of Disturbance Observer

K_{tn} are the robot mass, torque coefficient and their nominal values, respectively. Using a nominal model with an input signal and a measured output signal the disturbance observer estimates the equivalent disturbance defined as the nonlinear parameter variation, load disturbance, friction and then is utilized to cancel their effects. The performance of this estimation is determined by the bandwidth of the low-pass filter (**??**) which mainly reduces the high-frequency noise in the measured signal.

$$\hat{T}_{dis} = \frac{g_d}{s + g_d} T_{dis} \quad \cdots\cdots\cdots\cdots\cdots\cdots\cdots\cdots (45)$$

Increase in the cut-off frequency gain g_d of low-pass filter also increases the performance of disturbance estimation. It is possible to realize the acceleration based backstepping control method using disturbance observer. Block diagram of wheel control is given in Fig. **??**.

3.2 Control of Manipulator Manipulator part of the system has four degrees of freedom to control the position of the CoG. As a result, this system has redundancy. This redundancy is used to avoid singularities and increase the stability of null space motion.

In the redundant manipulator, joint space acceleration reference, obtained by using pseudo inverse matrix, can be written as (**??**). In this equation, first term represents the workspace acceleration motion and second term represents the null space motion.

$$\ddot{\boldsymbol{q}}^{ref} = \boldsymbol{J}_w^+(\ddot{\boldsymbol{x}}_{cog}^{ref} - \dot{\boldsymbol{J}}_w\dot{\boldsymbol{q}}) + (I - \boldsymbol{J}_w^+\boldsymbol{J}_w)\ddot{\boldsymbol{\phi}} \quad \cdots (46)$$

where $\boldsymbol{J}_w$ is the Jacobian matrix for the CoG position and $\boldsymbol{J}_w^+$ is the weighted pseudo inverse matrix and defined as

$$\boldsymbol{J}_w^+ = \boldsymbol{W}^{-1}\boldsymbol{J}_w^T(\boldsymbol{J}_w\boldsymbol{W}^{-1}\boldsymbol{J}_w^T)^{-1} \quad \cdots\cdots\cdots\cdots (47)$$

In the above equation, $\boldsymbol{W}$ is a diagonal weighting matrix. In the joint space disturbance observer based acceleration controller, $\boldsymbol{W}$ corresponds to the virtual inertia matrix $\boldsymbol{I}_{vn}$ and can be selected arbitrarily [(?)]. Since the base joint of the manipulator is passive and has different dynamic characteristics than the other links, $\boldsymbol{W}$ should be selected so that the passive joint does not affect the motion of the CoG in the workspace. This is possible if the element of $\boldsymbol{W}$ corresponding to the base joint element were selected as infinity. The structure of this matrix is shown in (**??**).

$$\boldsymbol{W} = \begin{bmatrix} w_{11} & 0.0 & 0.0 & 0.0 \\ 0.0 & 1.0 & 0.0 & 0.0 \\ 0.0 & 0.0 & 1.0 & 0.0 \\ 0.0 & 0.0 & 0.0 & 1.0 \end{bmatrix} \quad \cdots\cdots\cdots\cdots (48)$$

Here w_{11} is selected large enough to prevent the effect of the passive joint. The effect of the gain is checked easily by the simulation in advance.

Workspace and joint space disturbance observer are used in position control of the CoG to compensate the disturbance of the passive joint and other disturbance forces. By using the joint space and workspace observer, (**??**) can be rewritten as (**??**) without calculating the $\dot{\boldsymbol{J}}_w\dot{\boldsymbol{q}}$ and $(I - \boldsymbol{J}_w^+\boldsymbol{J}_w)$ terms [(?)].

$$\ddot{\boldsymbol{q}}^{ref} = \boldsymbol{J}_w^+\ddot{\boldsymbol{x}}_{cog}^{ref} + \ddot{\boldsymbol{q}}_{null}^{ref} \quad \cdots\cdots\cdots\cdots\cdots\cdots (49)$$

The acceleration reference of the CoG in the workspace motion $\ddot{\boldsymbol{x}}_{cog}^{ref}$ and in the null space are selected as

$$\ddot{\boldsymbol{x}}_{cog}^{ref} = \ddot{\boldsymbol{x}}_{cog}^{cmd} + \boldsymbol{K}_p(\boldsymbol{x}_{cog}^{cmd} - \boldsymbol{x}_{cog}) + \boldsymbol{K}_v(\dot{\boldsymbol{x}}_{cog}^{cmd} - \dot{\boldsymbol{x}}_{cog}) \quad (50)$$

$$\ddot{\boldsymbol{q}}_{null}^{ref} = -\boldsymbol{K}_{\boldsymbol{np}}\frac{\partial V(\boldsymbol{q})}{\partial \boldsymbol{q}} - \boldsymbol{K}_{\boldsymbol{nv}}\dot{\boldsymbol{q}} \quad \cdots\cdots\cdots\cdots (51)$$

where $\boldsymbol{K}_p$ and $\boldsymbol{K}_v$ are the proportional and differential gains of the manipulator in workspace, respectively. Taking the damping ratio $\zeta = 1$ (critically damped) $\boldsymbol{K}_p$ and $\boldsymbol{K}_v$ is determined by closed-loop characteristic polynomial as follows

$$\boldsymbol{K}_p = 2\omega M_n \quad \cdots\cdots\cdots\cdots\cdots\cdots\cdots (52)$$

$$\boldsymbol{K}_v = \omega^2 \quad \cdots\cdots\cdots\cdots\cdots\cdots\cdots\cdots (53)$$

where ω is the closed-loop natural frequency. In (**??**), first term is the null space vector for the avoidance of singularities, and second term is the velocity damping vector, used to increase the stability of null space motion [(?)]. $\boldsymbol{K}_{\boldsymbol{np}} \in R^3$ and $\boldsymbol{K}_{\boldsymbol{nv}} \in R^3$, respectively, are the constant gain parameters for the null space and velocity terms. The manipulability measure $V(\boldsymbol{q})$ that is defined as (**??**) is used for the performance criterion function to avoid singularities [(?)]. Manipulability measure takes values between one and zero. It only becomes zero when Jacobian matrix $\boldsymbol{J}_w$ losses rank (determinant of Jacobian is zero), which indicates a singular configuration. Thus, a zero manipulability measure can be utilized to avoid singular configurations.

$$V(\boldsymbol{q}) = \sqrt{det\left(\boldsymbol{J}_w\boldsymbol{J}_w^T\right)} \quad \cdots\cdots\cdots\cdots\cdots (54)$$

Block diagram of the CoG position control is given in Fig. **??**.

4. Experiment

4.1 Experimental setup To verify the validity of the proposed method, experiments were conducted on the two-wheeled mobile manipulator (Fig. **??**). The physical parameters of this system is given in Table **??**. In this system, encoders are used to measure the position of actuated joints and 3-dimensional dynamical angle-sensor (Datatec GU-3024) is used to measure the position and velocity of the passive joint. This device uses gyros and accelerometers to measure accelerations in three directions and, also the angular positions of pitch, roll and yaw with 60Hz output frequency. The serial port is used to communicate with this sensor and the counter board is used to read the value of encoders. The control program is written in C language, and executed using RT-Linux to control the system in real time environment. The sampling time is 1 ms.

4.2 Experimental Results Parameters of the proposed controller used during the experiments are selected as shown in Table **??**. Here K_{nv1}, K_{nv2}, K_{nv3} are the elements of velocity damping vector $\boldsymbol{K}_{nv}$ for the

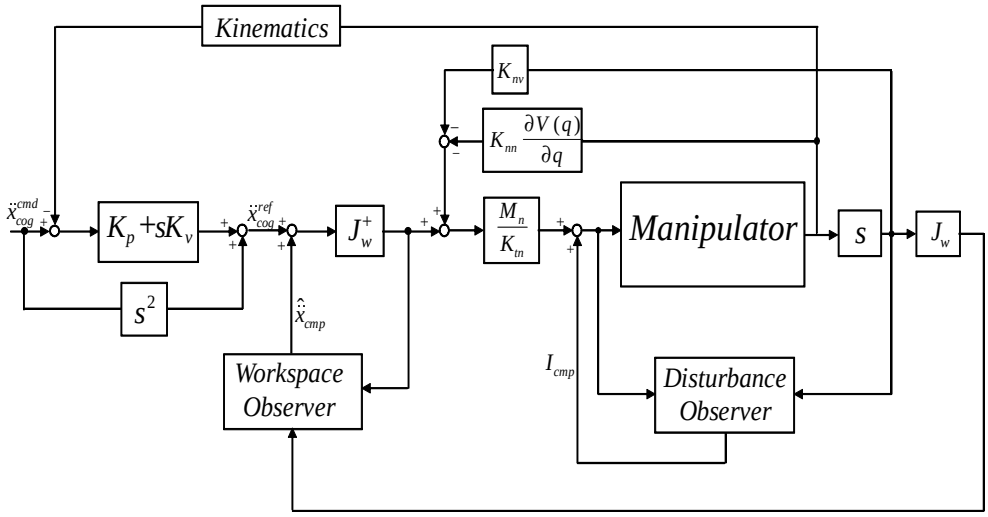

Fig. 7. Block diagram of manipulator control system

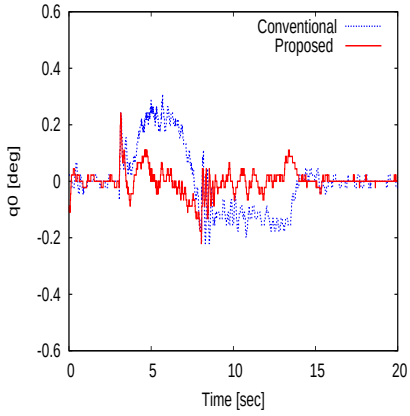

(a) Position response of the passive joint

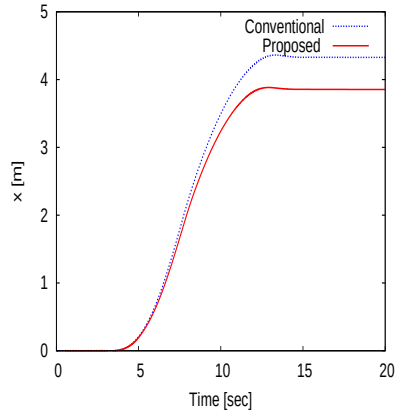

(b) Position response of the wheels in in ${}^{w}x$ direction

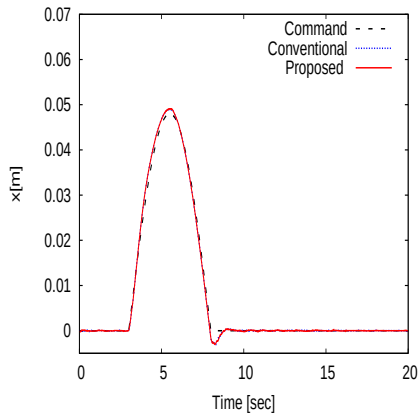

(c) The CoG position response of the manipulator in ${}^{v}x$ direction

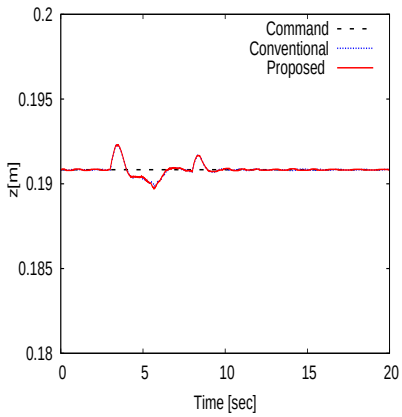

(d) The CoG position response of the manipulator in ${}^{v}z$ direction

Fig. 8. Experiment Result.

first, second, and third joints of the manipulator, respectively. The experiment results of proposed method are given together with the results of the conventional linear PD controller to demonstrate the efficiency of the proposed method. In the first experiment, the command for joint angle of the passive joint is set to zero degree and the CoG command for the manipulator is selected as

$$x_{cog}^{cmd} = \begin{cases} 0.0 & if \quad 0 \le t < 3 \\ 0.048\sin(0.2\pi(t-3)) & if \quad 3 \le t < 8 \\ 0.0 & if \quad 8 \le t \end{cases} \quad (55)$$

Joint angle response of the passive joint, the position response of the CoG in ${}^{v}x$ and ${}^{v}z$ directions can be seen in Fig. **??**(a), (b) and (c), respectively. These results indicate that the proposed nonlinear backstepping method can successfully stabilize the passive joint at zero degree

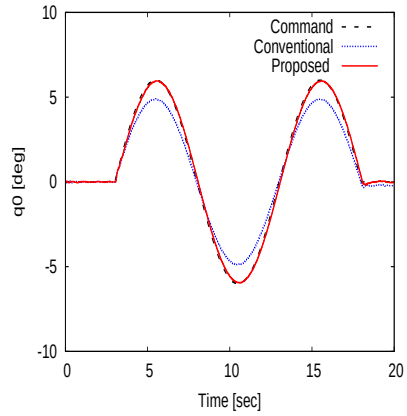

(a) Position response of the passive joint

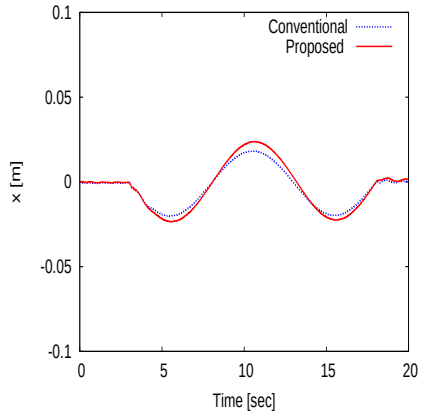

(b) Position response of the wheels in in ${}^{w}x$ direction

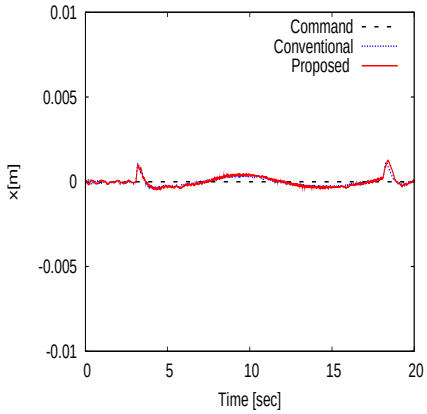

(c) The CoG position response of the manipulator in ${}^{v}x$ direction

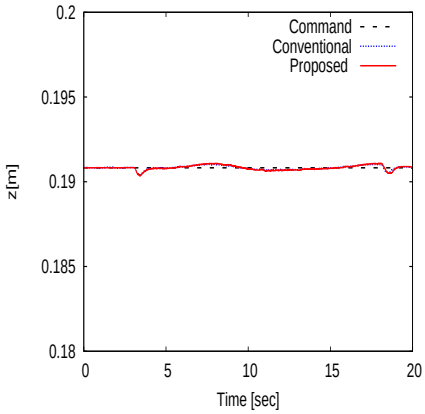

(d) The CoG position response of the manipulator in ${}^{v}z$ direction

Fig. 9. Experiment Result.

Table 3. Parameters of The Experimental System

m_0	Mass of the passive joint[kg]	7.2
m_1	Mass of the first link[kg]	1.06
m_2	Mass of the second link[kg]	0.84
m_3	Mass of the third link[kg]	0.25
R	Radius of the wheels[m]	0.20
W	Tread of the mobile base[m]	0.86
l_0	Length of the passive joint[m]	0.14
l_1	Length of the first link[m]	0.20
l_2	Length of the second link[m]	0.20
l_3	Length of the third link[m]	0.14

Table 4. The Experiment Parameters

Kp	Manipulator position control gain	225
Kv	Manipulator velocity control gain	30
K_{nv1}	Null space damping gain for the first joint	80
K_{nv2}	Null space damping gain for the second joint	20
K_{nv3}	Null space damping gain for the third joint	20
λ	Design parameter of Lyapunov function	40
c_1	Design parameter of Lyapunov function	7
c_2	Design parameter of Lyapunov function	20
K	Design parameter of Lyapunov function	1.0
ϕ	Thickness of saturation function	0.6
w_{11}	Element of weighting matrix	1000
g_d	Cut-off freq. of jointspace DOB [rad/s]	80
g_w	Cut-off freq. of workspace DOB [rad/s]	5
g_r	Cut-off freq. of rotational DOB [rad/s]	400
g_t	Cut-off freq. of translational DOB [rad/s]	400
q_1	Initial joint angle of the first joint [deg]	-30.0
q_2	Initial joint angle of the second joint [deg]	88.0
q_3	Initial joint angle of the thired joint [deg]	55.0

and the manipulator can track the given CoG command accurately. It is important to control the position angle of the passive joint precisely not only at zero degree but also at other degrees to take advantages of dynamical stability. In the statically stable manipulator, it is not possible to move the body without motion of wheels. Thus, the body does not have any effect on the manipulation task and force generation. On the other hand, in the two-wheeled mobile manipulator system by controlling the motion of the passive joint, the CoG of the manipulator can be moved over a greater range of positions, which increases the force generation ability of the manipulator. In the second experiment, instead of a constant joint angle, sine wave trajectory as given in (**??**) is used for the reference signal of the passive joint. The CoG command for the manipulator is set to zero in this experiment.

$$q_0^{cmd} = \begin{cases} 0.0 & if \quad 0 \leq t < 3 \\ 6.0\sin(0.2\pi(t-3)) & if \quad 3 \leq t < 18 \\ 0.0 & if \quad 18 \leq t \end{cases} \quad (56)$$

Fig. **??** (a), (b), and (c) give joint angle response of the passive joint, position response of the CoG of the manipulator in ${}^{v}x$ and ${}^{v}z$ directions, respectively. As seen from these results, passive joint follows the given sin wave trajectory command accurately.

The third experiment is conducted to illustrate the robustness of the proposed method against modeling errors. Since stability of the passive joint depends on its

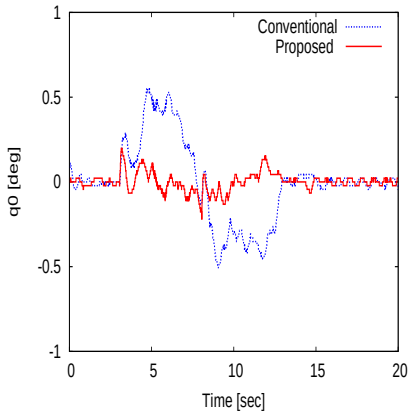

(a) Position response of the passive joint

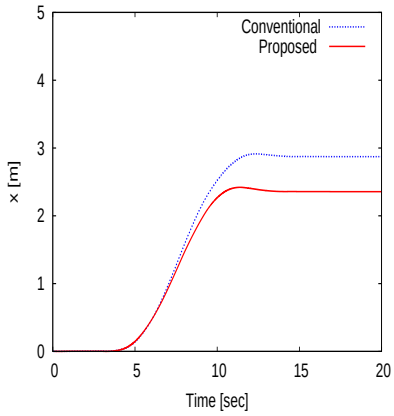

(b) Position response of the wheels in in ${}^{w}x$ direction

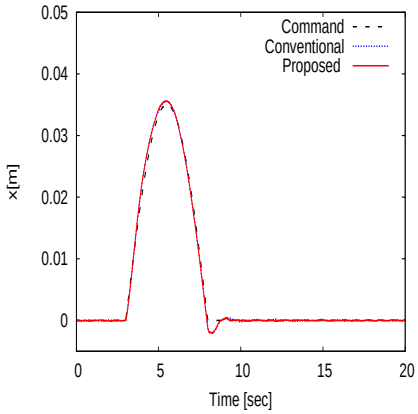

(c) The CoG position response of the manipulator in ${}^{v}x$ direction

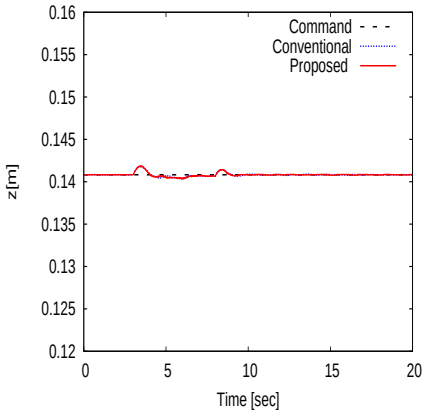

(d) The CoG position response of the manipulator in ${}^{v}z$ direction

Fig. 10. Experiment Result.

length, the length of the passive joint is used as a testing parameter to indicate the stability of the proposed method. Instead of its real measured value, 0.09m is used for the length of the passive joint. The command for joint angle of the passive joint is set to zero degree as in the first experiment. The CoG command of the manipulator is given as below

$$x_{cog}^{cmd} = \begin{cases} 0.0 & if \quad 0 \leq t < 3 \\ 0.035\sin(0.2\pi(t-3)) & if \quad 3 \leq t < 8 \\ 0.0 & if \quad 8 \leq t \end{cases} \quad (57)$$

Fig. **??** shows the result of this experiment. Even if there is a large modeling error, the proposed method achieves the stability of the passive joint.

5. Conclusion

In this paper, robust control of the two-wheeled mobile manipulator is realized. Due to the high degrees of freedom and highly nonlinear structure, the second, third and fourth links of manipulator are considered as one virtual link, which makes it possible to model this system as a double inverted pendulum. Then, backstepping with sliding mode based control design is proposed to regulate and track the motion of the passive joint in this model. In workspace, the CoG of position of the manipulator is controlled and manipulability measure is utilized as a performance index to avoid singularities in the null space. Several experiments were conducted on the two-wheeled mobile manipulator to confirm the validity of proposed method. The results of first two experiments demonstrate that it is possible to stabilize the passive joint at constant degree and track the given trajectory asymptotically. The last experiment indicates the efficiency of the proposed method in case of the modeling error. When the system is pushed to its limits, it may be reasonable to expect the actuator saturations. Although this paper does not take saturation into account in the design and analysis, it is possible to enhance the proposed method by implementing adaptive input saturation methods. This issue is considered as a future work.

References

(1) O. Brock, O. Khatib, and S. Viji, "Task-Consistent Obstacle Avoidance and Motion Behavior for Mobile Manipulation", *IEEE International on Robotics and Automation,* Vol. 1, 2002, pp. 388-393.

(2) K. Nagatani, and S. Yuta, "Designing Strategy and Implementation of Mobile Manipulator Control System for Opening Door", *IEEE International on Robotics and Automation,* Minneapolis, Vol.3, 1996, pp. 2828-2834.

(3) D. Katz, E. Horrell, Y. Yang, B. Burns, T. Buckley,A. Grishkan, V. Zhylkovskyy, O. Brock, and E. Learned-Miller "The UMass Mobile Manipulator UMan An Experimental Platform for Autonomous Mobile Manipulation", *Workshop on manipulation for human environments at robotics, science and systems,* Philadelphia, USA, August 2006.

(4) B. Browning, P. Rybski, J. Searock, and M. Veloso "Development of a soccer-playing dynamically-balancing mobile

robot", *In Proceedings of International Conference on Robotics and Automation (ICRA'04),* New Orleans, LA, May 2004.
(5) R. Brooks, L. Aryananda, A. Edsinger, P. Fitzpatrick, C. Kemp, U. O'Reilly, E. Torres-Jara, P. Varshavskaya, J. Weber "Sensing and Manipulating Built-For-Human Environments", *International Journal of Humanoid Robotics,* Vol. 1, No. 1, 2004, pp. 1-28.
(6) B. J. Thibodeau, P. Deegan, and R. Grupen "Static analysis of contact forces with a mobile manipulator", *Robotics and Automation, 2006. ICRA 2006. Proceedings 2006 IEEE International Conference*, Orlando, Florida, May 2006, pp. 4007-4012.
(7) H. G. Nguyen, J. Morrell, K. Mullens, A. Burmeister, S. Miles, N. Farrington, K. Thomas, and D. W. Gagee "Segway Robotic Mobility Platform", *Proc. SPIE Mobile Robots XVII,* Philadelphia, October 2004.
(8) K. Pathak, J. Franch, and S. Agrawal "Velocity and position control of a wheeled inverted pendulum by partial feedback linearization", *IEEE Trans. on Robot.,* vol.21, no.3, pp.505-513, Jun 2005.
(9) Y. Ha, S. Yuta "Trajectory Tracking Control for Navigation of an Inverse Pendulum Type Autonomous Mobile Robot" , *Proc. of the 1994 IEEE/RSJ International Conference on Intelligent Robots and Systems '94, IROS 94,* Munich, September 1994.
(10) H. Abe, and T. Murakami, "A Realization of Stable Attitude Control in Two Wheels Driven Mobile Manipulator", *Papers of Technical Meeting on Industrial Instrumentation and Control,* IEE Japan, 2006.
(11) M. Krstic, I. Kanellakopoulos, and P. V. Kokotovic, "Nonlinear and adaptive control design, Wiley, New York 1995.
(12) P. V Kokotovic, "The joy of feedback: Nonlinear and Adaptive", *IEEE Control System Magazine,* Vol. 12, No. 3, 1992, pp. 7-17.
(13) H. K. Khalil, "Nonlinear Systems, 3nd ed. Upper Saddle River, NJ,Prentice Hall , 2002.
(14) A. J. Koshkouei, and A. S. I. Zinober, "Adaptive backstepping control of nonlinear systems with unmatched uncertainty", Proceeding of the 39th IEEE Conference on Decision and Control American Control, Sydney, Vol. 5, December 2000, pp. 4765-4770.
(15) K. D. Young, V. I. Utkin, and U. Ozguner, "A Control Engineer's Guide to Sliding Mode Control", *IEEE Trans. on Control Systems Technology,* Vol. 7, No. 3, 1999, pp. 328・42.
(16) H.J. Shieh, and K. K. Shyu, "Nonlinear Sliding-Mode Torque Control with Adaptive Backstepping Approach for Induction Motor Drive", *IEEE Transaction on Industrial Electronics,* Vol. 46, No. 1, 1999, pp. 380-389.
(17) F. Lin, C. Chang, and P. Huang, "FPGA-Based Adaptive Backstepping Sliding-Mode Control for Linear Induction Motor Drive", *IEEE Transaction on Industrial Electronics,* Vol. 22, No. 4, 2007, pp. 1222-1231.
(18) H. Shieh, Y. Chiu, and Y. Chen, " A Filtered Switching-Type Sliding-Mode Backstepping Control Approach for a Piezopositioning Stage", *Proceedings of the 4th IEEE International Conference on Mechatronics*, Kumomoto, May 2007.
(19) K. Ohnishi, M. Shibata and T. Murakami, "Motion control for advanced mechatronics", *IEEE/ASME Trans. on Mechatronics,* Vol. 1, No. 1, 1996, pp. 56-67.
(20) K. Nakano, and T. Murakami, "An Approach to Guidance Motion by Gait-Training Equipment in Semipassive Walking", *IEEE Transaction on Industrial Electronics,* Vol. 55, No. 4, 2008, pp. 1707-1714.
(21) S. Tashiro, and T. Murakami, "Step Passage Control of a Power-Assisted Wheelchair for a Caregiver", *IEEE Transaction on Industrial Electronics,* Vol. 55, No. 4, 2008, pp. 1715-1721.
(22) J. Miyata, Y. Kaida, and T. Murakami, "$v - \phi$-Coordinate-Based Power-Assist Control of Electric Wheelchair for a Caregiver", *IEEE Transaction on Industrial Electronics,* Vol. 55, No. 6, 2008, pp. 2517-2524.
(23) J.E. Slotine, and W. Li, "Applied Nonlinear Control, Prentice-Hall", Englewood Cliffs, NJ, 1990.
(24) T. Yoshikawa " Foundation of Robotics: analysis and control", The MIT Press, 1990.
(25) N. Oda, T. Murakami, K. Ohnishi, " A Force Based Motion Control Strategy for Hyper-Redundant Manipulator", *23rd International Conference on Industrial Electronics, Control and Instrumentation(IECON'97),* Vol. 3, 1997, pp. 1285-1290.
(26) T.Murakami, K.Kahlen, and Rik.W.De Doncker, "Robust Motion Control based Projection Plane in Redundant Manipulator", *IEEE Transaction on Industrial Electronics,* Vol. 49, No. 1, 2002, pp. 248-255.
(27) N. Oda, T. Murakami, and K. Ohnishi, "Null Space Damping Method for Robust Controlled Redundant Manipulator", *IEEE 20th International Conference on Industrial Electronics, Control and Instrumentation(IECON'94),* Vol.2, 1994, pp. 755-759.

Cihan Acar (Non-member) received the B. E. degree in electrical and electronics engineering from Bilkent University, Ankara, Turkey in 2006 and the M. E. degree in integrated design engineering from Keio University, Yokohama, Japan, in 2008. He is currently a Ph.D. candidate at Keio University. His research interests are robotics, underactuated systems.

Toshiyuki Murakami (Senior Member) received the B. E., M. E., and Ph. D. degrees in electrical engineering from Keio University, Yokohama, Japan, in 1988, 1990, and 1993, respectively. In 1993, he joined the Department of Electrical Engineering, Keio University, where he is currently a Professor in the Department of System Design Engineering. From 1999 to 2000, he was a Visiting Researcher with The Institute for Power Electronics and Electrical Drives, Aachen University of Technology, Aachen, Germany. His research interests are robotics, intelligent vehicles, mobile robots, and motion control.

View publication stats